Rock-weir fishway II: design evaluation and considerations

Abul Basar M. Baki, David Z. Zhu, Andrew Harwood, Adam Lewis & Katie Healey

Published online: 11 Sep 2017.

Submit your article to this journal ⎘

View related articles ⎘

View Crossmark data ⎘

Taylor & Francis
Taylor & Francis Group

IWHR

Rock-weir fishway II: design evaluation and considerations

Abul Basar M. Baki[a], David Z. Zhu[b], Andrew Harwood[a], Adam Lewis[a] and Katie Healey[a]

[a]Ecofish Research Ltd., Vancouver, Canada; [b]Department of Civil and Environmental Engineering, University of Alberta, Edmonton, Canada

ABSTRACT

The flow characteristics of a rock-weir type nature-like fishway are determined by the configuration of the stream channel and passage structures. For a fishway to be effective, the rock-weir hydraulics must be compatible with the swimming capabilities of the target fish species. This study optimized the design characteristics of rock-weir fishways by simulating the water depth and velocity for different channel characteristics and geometries, which govern the fish resting zones, volumetric dissipated power and ultimately upstream fish passage performance. This study provided recommendations on effective pool spacing, bed slope, weir height, weir angle and weir arrangements for designing rock-weir fishways. These design recommendations are based on fishway hydraulics and should provide suitable hydraulics for fish migration and sufficient slow velocity areas for fish resting in rock-weir fishways for specific structure geometries and channel characteristics.

1. Introduction

Nature-like fish passes (NLFs) are similar to a steep natural river reach linking upstream and downstream reaches, which generally require the installation of large rocks to dissipate energy, reduce flow velocities and increase water depth to mimic riverine habitats (Franklin et al. 2012). NLF designs generally fall into two categories: pool-weir type and rock-ramp type (Katopodis and Williams 2011). Pool-weir fishways are constructed using a series of weirs and pools in a stepped fashion, rather than having a single large drop (Katopodis and Williams 2011). Pool-weir type NLF structures are designed in consideration of fish passage goals and the physical setting; common structures include rock-weirs, step-pools and crossbar block ramps. The rock-weir fishway is very similar to engineering pool-type fishways and the design criteria are fairly comparable (Baudoin et al. 2014). Rock-weirs are composed of boulders in rows at regular intervals to form a series of pools. The result is a set of virtual pools due to the retention effect of weirs, where fish are likely to find resting zones (Baudoin et al. 2014).

The available guidelines related to rock-weirs are limited, primarily site specific (Cox 2005) and do not provide general design guidance for hydraulic performance. Thomas et al. (2000) and Rosgen (2001) suggest conceptual designs for rock-vortex structures (rock-weir in U-shape), DVWK (2002) provides some guidelines for bottom block ramps (rock ramp and rock-weir) and Baudoin et al. (2014) proposed pre-assessment procedures for rock-chutes/weirs (staggered arrays and successive rows of rock). However, none of these efforts have linked the hydraulics produced by the channel and structure configurations to fish passage performance, and hence there is no general design guideline for rock-weir fishways.

To provide design guidelines, this study systematically defines the effects of channel and structure configurations on rock-weir hydraulics to optimize the design for fish passage. This work builds on Baki et al. (2017) in part I, which developed general relationships for the depth-discharge and velocity predictions for rock weir fishways. The specific objectives of this study are to: 1) examine the effects of channel characteristics and structure geometries on flow depth and velocity, 2) interpret fishway hydraulics in the context of fish passage and 3) develop a procedure to guide the design of rock-weir fishways.

2. Numerical modelling approach

Baki et al. (2017) in part I investigated the hydraulics of rock-weir fishways for three different weir layouts: (I) V-weir facing upstream, (II) V-weir facing downstream and (III) crossbar block ramp (Figure 1). Numerical simulations were completed for different weir structure geometries (pool spacing L, weir height d and arm angle θ) and channel characteristics (bed slope S_0 and flow rate Q); these simulations are described in detail in Baki et al. (2017) based on Figure 1.

The numerical simulations were conducted using the commercial software ANSYS-CFX (2015), and the model performance was validated with a series of
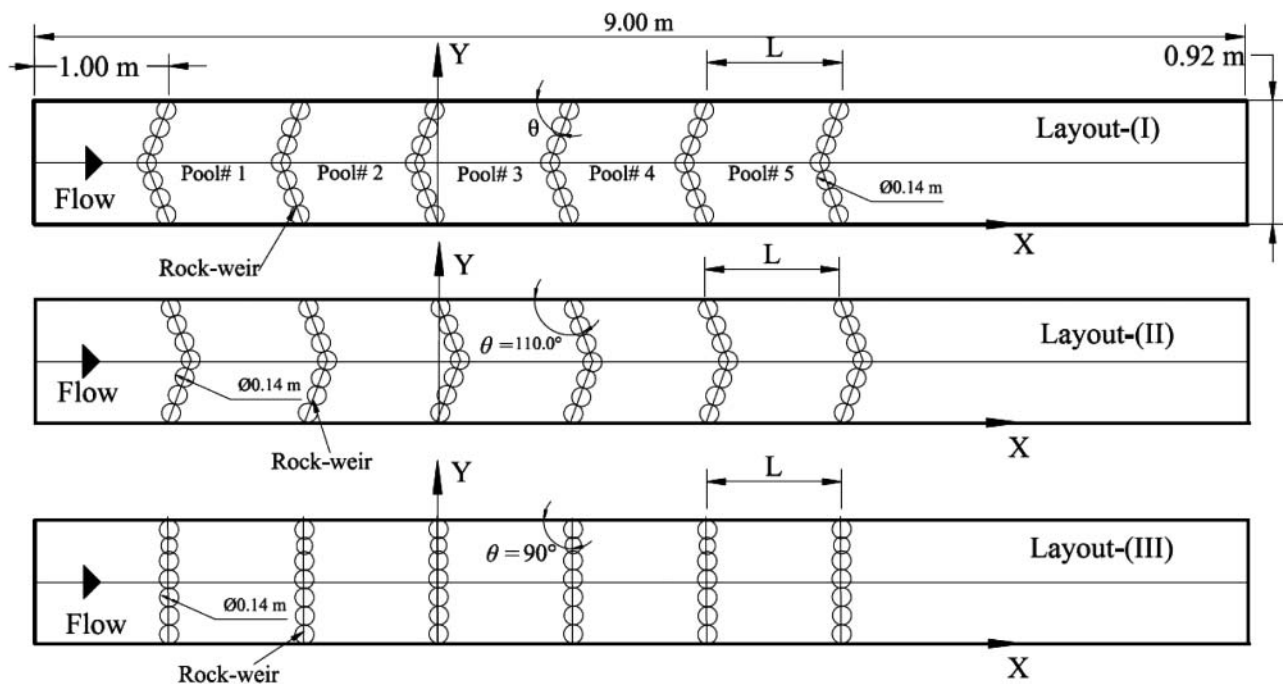

CONTACT Abul Basar M. Baki ✉ baki@ualberta.ca

Figure 1. Rock-weir layouts for CFD model domain: Layout I (V-weir facing upstream), II (V-weir facing downstream) and III (cross-bar block ramp). (adapted from Part I, Baki et al. 2017).

experimental observations for water depth and velocity; good agreement was achieved. A complete outline of the model, model development, corresponding boundary conditions and model validation is available in Baki et al. (2017) part I.

3. Results and discussions

3.1. Water depth

The effects of channel and structure configurations on pool water depths were quantified by calculating the ratio of water depths for the channel with and without the weirs (Figure 2). The simulated average water depth, H, was calculated along the centre line of the channel and the unregulated water depth, H_0, (without weir, referred to as normal depth) was calculated using Manning's equation (assuming $n = 0.012$, corresponding to a smooth steel bottom). It is noted that here H is a simplified smooth bed in a rectangular channel, and will vary with the downstream channel geometry *in situ*, resulting in different channel hydraulics. The presence of the weir structures in the fishway resulted in pool depths of 3.0–5.6 times normal depth. When flow rates were increased from 0.03 to 0.15 m³s⁻¹ in series A, this ratio decreased from 5.0 to 3.5, because the flow regime changed from weir to transitional and then streaming at higher flow rates (more details on flow regimes are described in Baki et al. 2017). Comiti et al. (2009) found that the water depth in step-pools differs significantly from weir to streaming flow regimes due to changing channel total roughness. Increasing the bed slope from 1.5% to 10% (Series B

and $Q = 0.06$ m³s⁻¹) resulted in increased ratios (from 3.9 to 4.9 times normal depth). As the pool spacing increased from 0.5 to 2B, the ratio decreased rapidly from ∼ 4.6 to 4.0, with slower rates of increase observed for spacing greater than 2B (constant $S_0 = 3\%$ and $Q = 0.06$ m³s⁻¹). For the larger pool spacing, the rock-weir water depth converged to nearly normal depth due to a decrease in boulder density, where boulder density is the fraction of the bed area occupied by boulders projected on the horizontal plane. Increasing weir height from 0.065 to 0.185 m resulted in a large increase in pool water depths, from 3.0 to 5.6 times normal depth ($S_0 = 3\%$ and $Q = 0.06$ m³s⁻¹), which is expected because of a taller weir results in a higher hydraulic control and hence more backwatering. The weir arm angle had a minor impact on ratios of pool water depth; the ratio relative to normal depth decreased by 0.25 when arm angle (θ) was reduced from 70 to 45 degrees ($S_0 = 3\%$ and $Q = 0.06$ m³s⁻¹ and $L = 1.5B$).

Figure 3 presents the pool average water depth (H) in full-scale fishways as a function of specific discharge q (flow rate per unit channel width, m²s⁻¹) for different channel and structure configurations, where the model-to-prototype scale is 1:4 following Baki et al. (2014). These depths were compared to recommended threshold values of $H = 0.5$ m and 0.2 m for salmonid and cyprinid species (Baudoin et al. 2014), to evaluate the performance of different designs. For all simulations of the full-scale fishway, H ranged from 0.41 to 1.15 m, corresponding to specific discharges that ranged from 0.26 to 1.33 m²s⁻¹. H satisfies the recommended minimum pool average water depth for
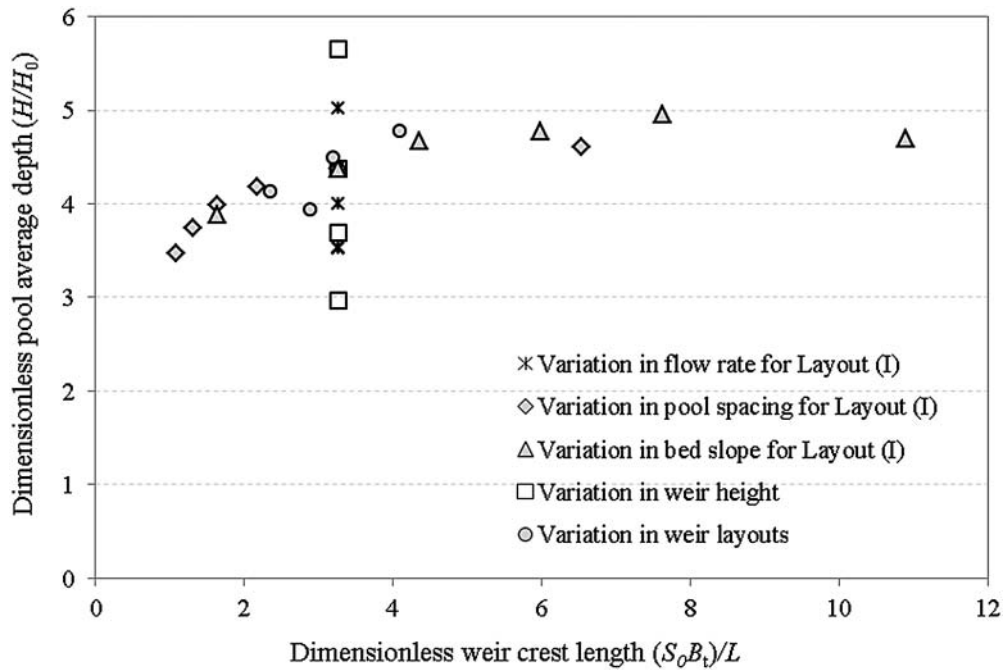
Figure 2. Pool average water depth associated with variations of flow rate, pool spacing, bed slope, weir height and weir layouts. The simulated average water depth, *H*, was calculated along the centre line of the channel and the unregulated water depth, H_0, (without weir, referred to as normal depth) was calculated using Manning's equation (assuming $n = 0.012$, corresponding to a smooth steel bottom).

salmonids of 0.5 m for all configurations except B5, C5 and E1 at 0.35 $m^2 s^{-1}$, and satisfies the minimum 0.2 m for cyprinid species for all configurations (Figure 3). In B5 ($S_0 = 10\%$) and C5 ($L = 3B$), the rock-weir water depth converged to nearly normal depth (as mentioned above). For E1 ($d = 0.065$ m), *H* does not satisfy the recommended depth of 0.5 m for salmonids due to the decrease in flow resistance at higher submergence ($H/D > 1.5$).

3.2. Flow velocity

The relationships between channel and structure configurations and the maximum velocity reduction factor ($\eta = 100 \times (V_0 - U_{max})/V_0$) are shown in Figure 4. V_0 is the pre-structure velocity that is present at normal depth. Increasing the flow rate from 0.03 to 0.15 $m^3 s^{-1}$ resulted in η decreasing from 45% to 37% (series A). Increasing bed slope from 1.5% to 10%
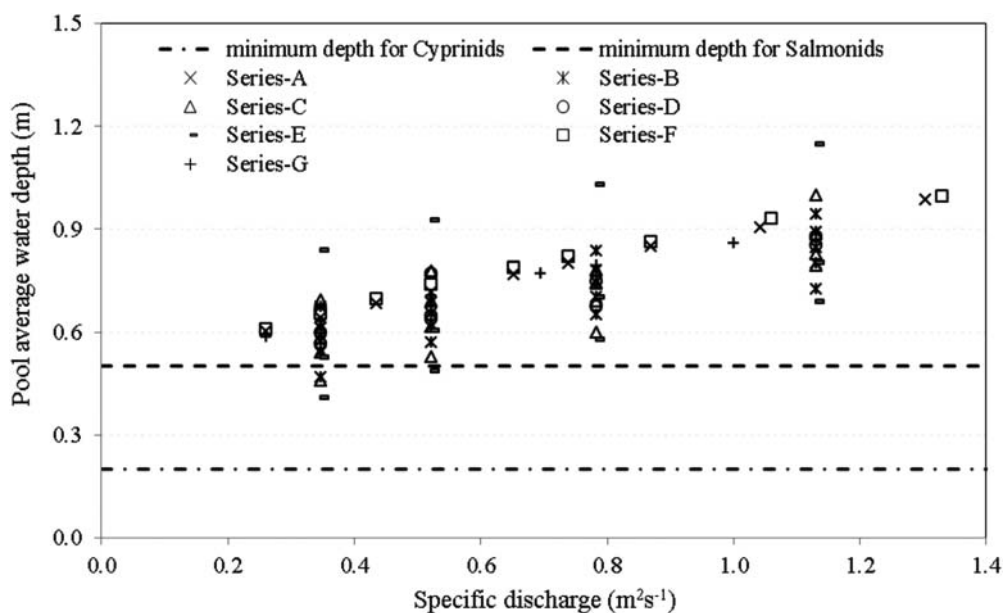

Figure 3. Pool average water depth in a full-scale fishway (1:4) as a function of flow rate per unit channel width (specific discharge) for different channel and structure configurations (horizontal dashed lines are the recommended minimum values for salmonids (*H* = 0.50 m) and cyprinids (0.20 m)).
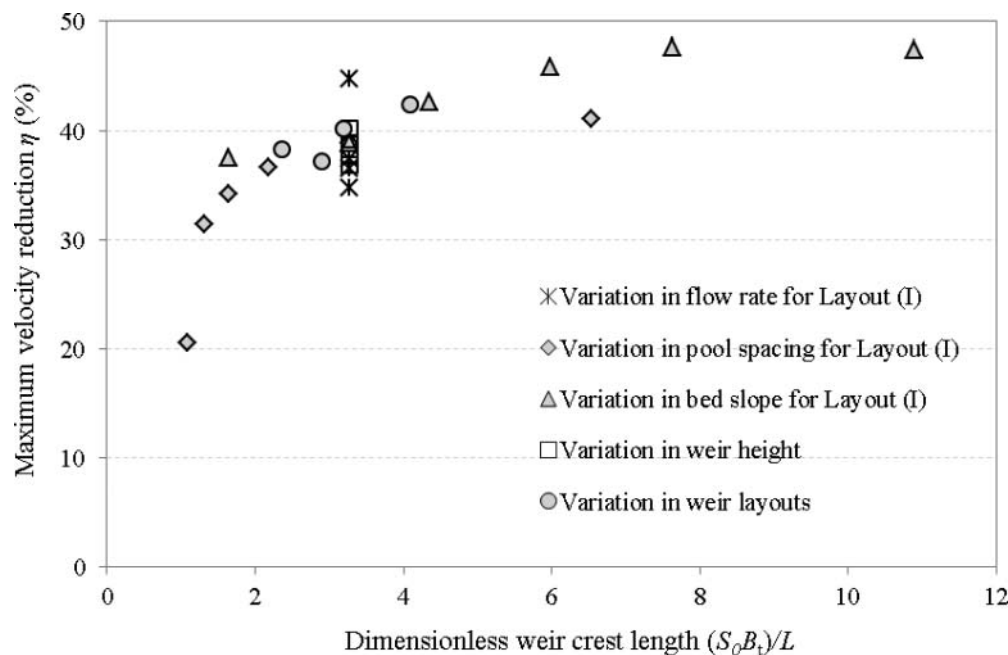
Figure 4. Maximum velocity reduction η associated with variations of flow rate, pool spacing, bed slope, weir height and weir layouts.

resulted in η increasing from 38% to 47% ($Q = 0.06$ m³s⁻¹). These findings are consistent with expectations that η decreases with increasing flow rate and increases with increased bed slope. For a rock-ramp fishway, Baki et al. (2014) found a 9% decrease in η as flow rate was increased from 0.06 to 0.16 m³s⁻¹ and an 8% increase in η as slope increased from 1.5% to 5%. The η value for the shorter pool spacing ($0.5B$) is about 21% greater than for the longer pool spacing ($3B$): η decreases gradually with increased spacing from 0.5 to $2.5B$ (10%), and decreases by an additional 11% due to increased spacing from 2.5 to $3B$ ($Q = 0.06$ m³s⁻¹, $S_0 = 3\%$). For the pool spacing $3B$ and larger, the post-structure maximum velocity converged to closely mimic pre-structure velocity corresponding to the normal depth due to a decrease in boulder density (as mentioned above). Increasing the weir height from 0.065 to 0.185 m had minimal effect on the velocity reduction factor: η only increased 2% from 37% to 39% ($S_0 = 3\%$, $Q = 0.06$ m³s⁻¹).

The η was relatively insensitive to weir layout: simulations for V-weirs facing both upstream (layout I) and downstream (layout II) produced a similar value ($\eta \sim 40\%$) ($S_0 = 3\%$, $Q = 0.06$ m³s⁻¹). The η for layout (III) was about 42%, similar to layout (I) ($S_0 = 4\%$, $Q = 0.06$ m³s⁻¹). Similarly, arm angle (θ) had little effect on η; η increased by 2% as θ decreased from 70 degrees to 45 ($S_0 = 3\%$ and $Q = 0.06$ m³s⁻¹, $L = 1.5B$).

3.3. Slow velocity zones

Zones of slow velocity are important for fish resting. The availability of these zones for different channel and structure configurations was examined by

calculating the frequency distributions of relative (dimensionless) velocities (U/U_{max}) in a horizontal plane at $z = 0.5H$ (Figure 5), assuming that the target fish species typically like to swim in a horizontal plane at $z = 0.5H$. The results of this analysis are independent of discharge (Wang et al. 2010); results are presented only for 0.06 m³s⁻¹ simulations but are also applicable to other discharge conditions. These frequency distributions provide an estimate of the average percentage of the pool area (slow velocity zones) present in the horizontal plane, where fish will rest for short periods without expending excessive energy (Wang et al. 2010). For the engineered pool-weir fishway, Bell (1986) suggested that velocity must be kept under 0.3 ms⁻¹ in 30%–50% of the volume of the pool. Assuming that the velocity must be kept under $0.4U_{max}$ (Baki et al. 2016), the simulated results for rock-weir NLFs confirmed that the average percentage of areas where the velocity is lower than $0.4U_{max}$ range from 23% to 38% for series-A4 and B1–B5 (Figure 5(a)) ($S_0 = 1.5\%$ to 10%), 32%–48% for series-C1–C5 (Figure 5(b)) ($L = 0.5–3B$), 5%–64% for series-E1–E3 (Figure 5(c)) ($d = 0.065–0.185$m) and 28% to 42% for series-, D1–D2, F4 and G3 (Figure 5(d)) (layouts (I)– (III)). The areas of slow velocity (less than $0.4U_{max}$) increased from 23% to 38% as channel slope increased from 1.5% to 5.5%, and declined to 25% as slope increased to 10% (Figure 5 (a)). Wang et al. (2010) also observed that the resting zone decreases significantly when the slope increases from 5% to 15%. Increasing pool spacing from 0.5 to $2.5B$ increased resting areas from 29% to 48%, the increase from 2.5 to $3B$ resulted in a decline to 35% (Figure 5(b)). Increasing the weir height influenced the resting zones substantially (Figure 5(c)). The area
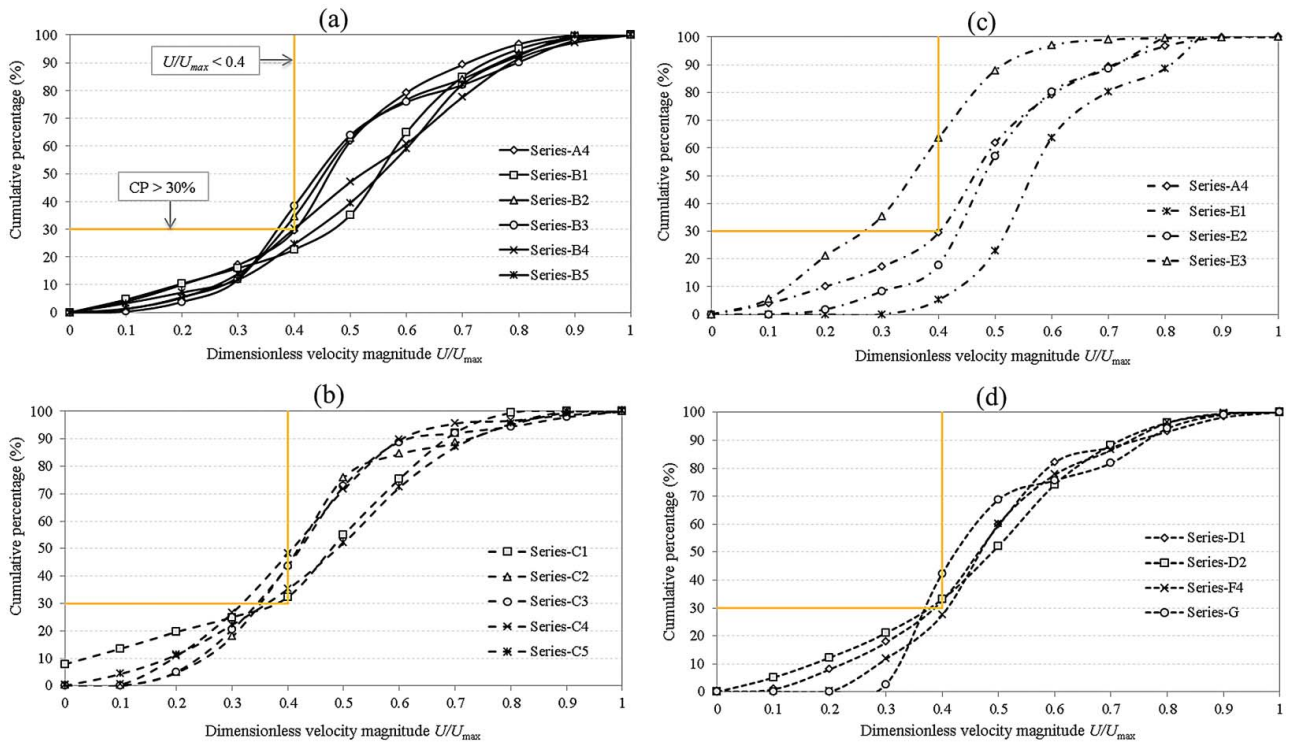
Figure 5. Cumulative frequency distribution of dimensionless velocity magnitude U/U_{max} on the horizontal plane at $z = 0.5H$ in the pool associated with variations of (a) bed slope, (b) pool spacing, (c) weir height and (d) weir layouts at 0.06 m^3s^{-1} (reference lines highlighted the area for $U/U_{max} < 0.4$ and cumulative percentage, CP > 30%).

under $0.4U_{max}$ increased from 5% to 64% as weir height was increased from $d = 0.065$ m to $d = 0.185$ m. The orientation of the V-weir has a negligible effect on the availability of slow velocity zones (Figure 5(d)): the average percentage of areas $< 0.4U_{max}$ is the same ($\sim$30%) for layouts (I) and (II) ($S_0 = 3\%$, $L = 1.0B$). Layout (III) (crossbar block) has about 10% more area under $0.4U_{max}$ than layouts (I) and (II). Similarly, the arm angle (θ) has little effect on the availability of slow velocity zones: both D1 ($\theta = 60$ degrees) and D2 ($\theta = 45$ degrees) have $\sim$33% area under $0.4U_{max}$ ($S_0 = 3\%$, $L = 1.5B$). In summary, sufficient resting areas (i.e. zones where the velocity is less than $0.4U_{max}$ over 30% of the pool area) are predicted to be present for bed slope $S_0 \leq 5.5\%$, pool spacing $L \leq 2.5B$ and weir height $d \geq 0.125$ m.

3.4. Energy dissipation rate

Pool type fishways are designed to cause energy dissipation and to provide lower current velocity and higher water depth in the downstream pool section while maintaining acceptably low levels of turbulence (Towler et al. 2015). The average volumetric energy dissipation rate (E) in a pool is calculated using the following basic formula.

$$E = \frac{\rho g Q \Delta h}{V_P} \tag{1}$$

where V_p is the volume of pool excluding the volume of the rock-weir. The relationship between E and q (flow rate per unit channel width or specific discharge) is presented for the study channel and structure configurations in Figure 6. E generally increases with specific discharge; for example, E increases from 63 to 198 Wm^{-3} as specific discharge increases from 0.033 to 0.163 m^2s^{-1} in Series A ($S_0 = 3\%$). This is consistent with the findings of Yagci (2010), who found E increased with increasing discharge at a constant bed slope for a pool-weir fishway.

E increases by an order of magnitude as channel slope is increased from 1.5% to 10%, from 54 to 519 Wm^{-3} (at $q = 0.065$ m^2s^{-1}). This agrees with the findings of Wu et al. (1999), who showed that E increased with the slope of a vertical slot fishway. Similarly, E is also sensitive to weir height. E increases by about 76% when d is increased from 0.065 to 0.185 m. The results demonstrate that structure geometry (pool spacing L and arm angle θ) has a modest influence on average volumetric energy dissipation rate compared to channel characteristics (flow rate and channel slope). E increases approximately 32% as pool spacing increased from $L = 1.0B$ to $3.0B$ (at $q = 0.065$ m^2s^{-1}). As arm angle was decreased from $\theta = 70$ degrees to 45 degrees, E increases approximately 22% (at $q = 0.065$ m^2s^{-1}). Weir layouts have minimal influence on E: changing V-weir layouts from upstream facing (layout I) to downstream facing (layout II) increased E by $\sim$ 5% (at $q = 0.065$ m^2s^{-1} and $S_0 = 3\%$),
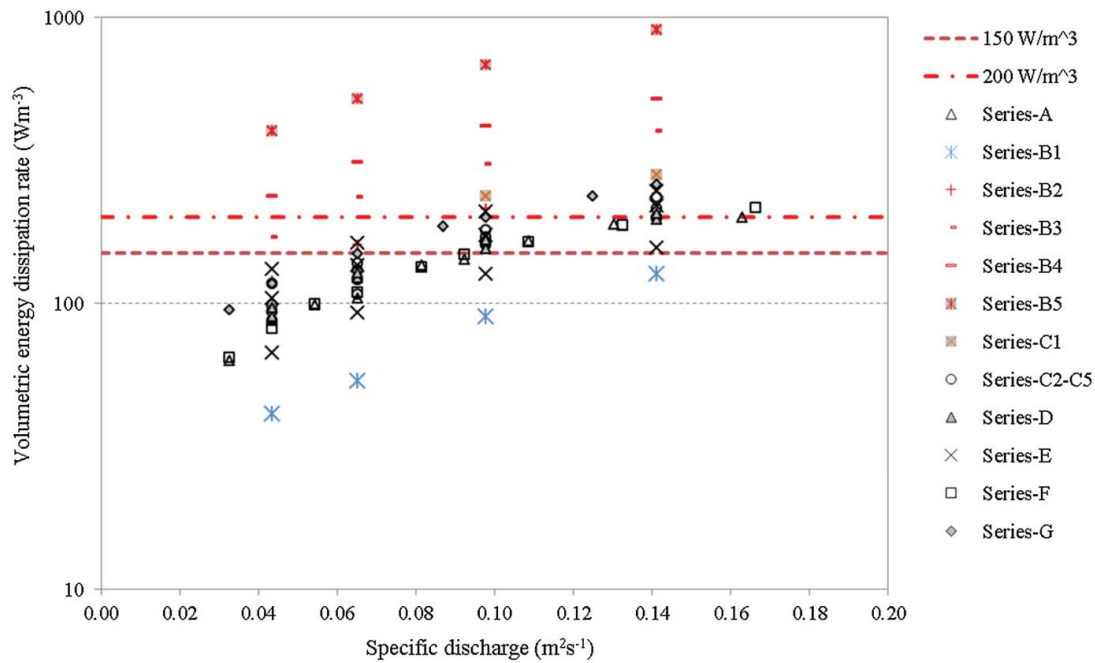
Figure 6. Relationship between average volumetric energy dissipation rate E and flow rate per unit channel width (specific discharge) for all simulations.

and changing from upstream facing (layout I) to cross-bar block ramp (III) decreased E by 7% (at $q = 0.065$ m²s⁻¹ and $S_0 = 4$%).

The exponent in a power relationship between volumetric power dissipation and specific discharge is approximately 2/3 for all series, except B1, C1 and E1. For B1 ($S_0 = 1.5$%) and C1 ($L = 0.5B$), this exponent is close to 1 (i.e. the E versus q relationship is approximately linear) because a streaming flow regime is present, which is dominated by recirculation eddies and air concentration rather than uniform distribution of velocity over depth (Toombes 2002). The exponent is close to $^1/_2$ for E1 ($d = 0.065$ m) as higher submergence ratios cause lower form drag, leading to reduced energy dissipation.

According to Larinier (2008), the average volumetric energy dissipation rate should not exceed 200 Wm⁻³ for large salmon and sea trout and 150 Wm⁻³ for smaller shad and riverine species. For the simulated results of series B2–B5 and C1, the average volumetric energy dissipation rates are mostly above both criteria of 150 and 200 Wm⁻³, and series-A, B1, C2–C5, D1–D2, E1–E3, F and G are typically within the energy dissipation criteria (Figure 6) except at the greatest specific discharge of 0.14 m²s⁻¹. These results could be applied *in-situ* for a small stream on a 1:1 Froude model scale. For a full-scale structure (prototype), where the model-to-prototype scale is 1:4, the average volumetric energy dissipation rates for the series-C1–C4, D1–D2, E2 and G are below the lower limit of 150 Wm⁻³ at a specific discharge q of 0.043 m²s⁻¹ or less, and series-A, B1, E1 and F are below the upper limit of 200 Wm⁻³ at $q = 0.065$ m²s⁻¹ or less.

3.5. Fish swimming performance

The swimming performance of target fish species is a primary consideration in fishway design: the effectiveness of fishway hydraulics depends on both fish swimming speed and endurance, i.e. the length of time during which the fish can maintain a specific speed (Puertas et al. 2012). In general, fish movement is characterized by three different swimming speeds: burst/sprinting speed (maintained for a short time, ranging from a few seconds to a few dozen seconds (Baudoin et al. 2014), less than 20 seconds (Katopodis and Gervais 2012)); sustained speed (maintained for a few minutes up to 10 or 12 minutes (Baudoin et al. 2014), around 30 minutes (Katopodis and Gervais 2012); and cruising speed (indefinitely) (Baudoin et al. 2014). Because fish movements are not independent of scale, this study analyses fish swimming performance for a full-scale structure (prototype) where the model-to-prototype scale is 1:4.

Puertas et al. (2012) recommend the application of two fatigue restrictions related to the velocity field. The first restriction states that the maximum flow velocity cannot exceed the fish burst speed (assumed to be 10 body lengths per second, or "$10L_B/s$ rule for burst capacity", per Hammer 1995), i.e. $U_{max} \leq$ burst speed. This restriction limits the value of $S_0 \times L$ (bed slope × pool spacing) using dimensionless maximum velocity, $U_{max}^* = U_{max}/\sqrt{2gS_0L}$. Solving the first velocity restriction $10L_B/s \geq \sqrt{2gS_0L} \times U_{max}^*$ for a specific (e.g. 200 mm) body length of salmonids or cyprinids provides the allowable pool spacing as a function of maximum
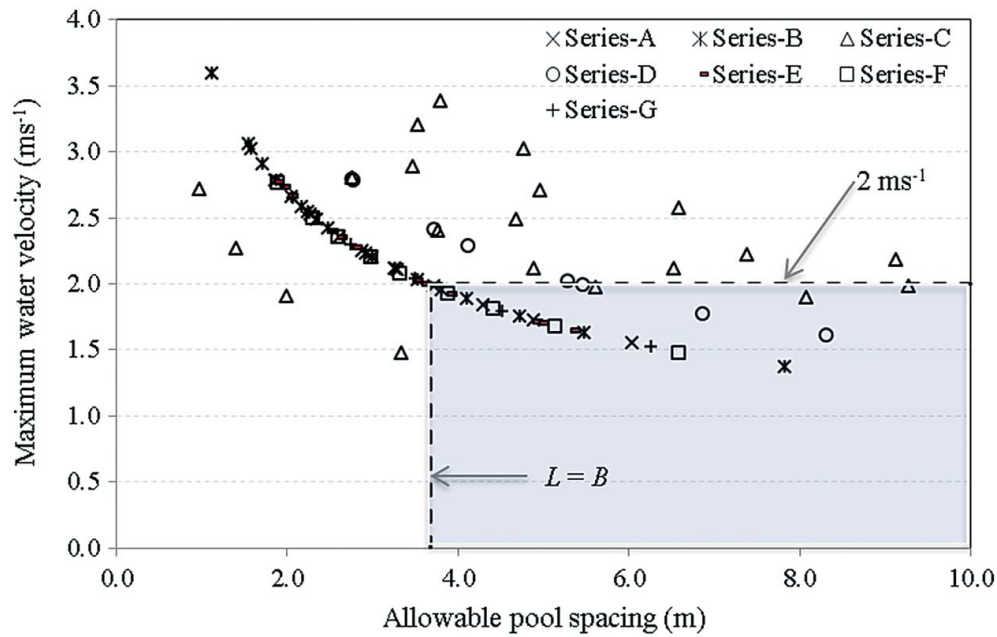
Figure 7. Relationship between maximum water velocity and allowable pool spacing at a prototype scale for 200-mm body length of salmonids or cyprinids. The dashed lines show $U_{max} \leq 2.0$ ms^{-1} (horizontal) and $L \geq B$ (vertical).

water velocity in prototype rock-weir fishways; this relationship is shown in Figure 7 for all simulations.

For 200-mm salmonids or cyprinids, an effective fishway design has to meet the requirements of $U_{max} \leq 2.0$ ms^{-1} (equivalent to the burst swimming speed of 200-mm salmonids or cyprinids) and allowable pool spacing $L \geq B$ (at least channel width). This assumption is similar to DVWK (2002) and Larinier (2008), who recommended that maximum water velocity in a fishway typically should not exceed 2.0 ms^{-1} for different fish species. Following the first restriction in Figure 7, the maximum flow velocities in all simulations of series-A, B, C, D, E, F and G at a flow rate of 1.92 m^{3}s^{-1} (equivalent to 0.06 m^{3}s^{-1} in the model) or less in the prototype achieve the above requirements (Table 1). Here, the maximum velocities for the simulations in series-B ($S_0 = 5.5\%$–7%), C ($L = 1.5$–2.5B) and E ($d = 0.065$–0.095 m) restricted the fish swimming performances at higher flow rates ($Q > 1.28$ m^{3}s^{-1}). The simulations for B5 ($S_0 = 10\%$), C1 ($L = 0.5B$) and C5 ($L = 3B$) did not meet the requirement of $U_{max} \leq 2.0$ ms^{-1} for any flow rate.

The second restriction is related to the effort required for a fish to swim along a path without resting (Puertas et al. 2012) in consideration of variable water velocity along the path. This restriction limits the maximum fish swimming distance, D_{max}, against an equivalent constant water velocity, U_{eq}, equivalent to the average velocity along the fish path (Puertas et al. 2012). Puertas et al. (2012) applied optimization to the endurance formulae suggested by Castro-Santos (2005) (Equation 2) to obtain the maximum distance D_{max} (cm) that the fish can swim against an equivalent velocity U_{eq} (Equation (3))

Table 1. Swimming performance of salmonid and cyprinid species for the first fatigue restriction.

Weir layouts	Series (simulation)	Flow rate[a] (m^{3}s^{-1})	Fish species (200-mm body length)	First restriction[*]	
				Successful	Unsuccessful
I	A	1.92	Salmonids or Cyprinids	√	
I	B1–B2	1.92	Salmonids or Cyprinids	√	
I	B3–B4	1.28	Salmonids or Cyprinids	√	
I	B5	1.28	Salmonids or Cyprinids		√
I	C1	1.28	Salmonids or Cyprinids		√
I	C2–C4	1.28	Salmonids or Cyprinids	√	
I	C5	1.28	Salmonids or Cyprinids		√
I	D1–D2	1.92	Salmonids or Cyprinids	√	
I	E1	1.92	Salmonids or Cyprinids	√	
I	E2–E3	1.28	Salmonids or Cyprinids	√	
II	F	1.92	Salmonids or Cyprinids	√	
III	G	1.92	Salmonids or Cyprinids	√	

[a]Maximum flow rate in prototype model (1:4 scale).
[*]$U_{max} \leq 2.0$ ms^{-1} and $D_{max} \geq L$.

$$D_f = (a(L_B)^b + c\ln(T) - U_{eq})T \qquad (2)$$

$$D_{max} = -c.\exp\left(\frac{U_{eq}}{c} - \frac{a}{c}(L_B)^b - 1\right) \qquad (3)$$

where T is the endurance time in seconds and a, b and c are coefficients that depend on the fish species and water temperature (for more details see Puertas et al. 2012). The coefficients for the endurance–velocity formulae for salmonids are: $a = 17.31$, $b = 0.47$ and
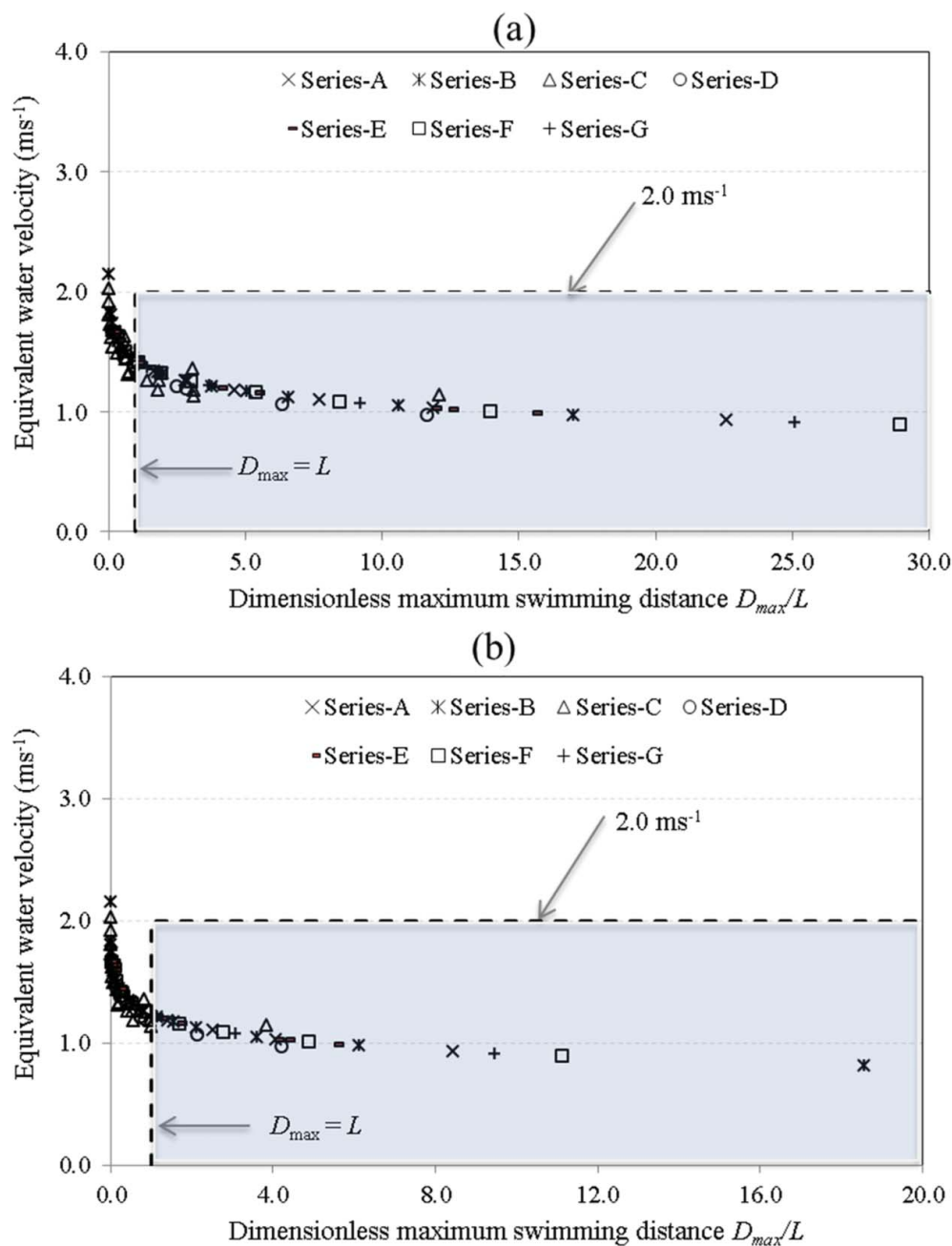
Figure 8. Relationship between equivalent water velocity and dimensionless maximum swimming distance (D_{max}/L) in a prototype scale for 200-mm body length of (a) salmonids and (b) cyprinids. The dashed lines show $U_{eq} \leq 2.0$ ms^{-1} (horizontal) and $D_{max} = L$ (vertical).

$c = -16.02$, and for cyprinids are $a = 30.34$, $b = 0.34$ and $c = -14.29$ (Puertas et al. 2012).

Adopting the above endurance–velocity formulae as fatigue curves, the relationship between maximum fish swimming distance (D_{max}) and equivalent water velocity in a prototype fishway for 200-mm body length of salmonids and cyprinids is shown in Figure 8 for all simulations. Similar to the first restriction, the effective design of a fishway has to meet the requirements of $U_{eq} \leq 2.0$ ms^{-1} and maximum swimming distance, $D_{max} \geq L$ (at least one pool length) for a 200-mm salmonid or cyprinid. Figure 8(a) shows that the prototype flow fields in almost all of the simulations achieve the above requirements for salmonids (Table 2) at a flow rate 3.20 m^{3}s^{-1} or less (in prototype). The

swimming performance for cyprinids is very sensitive to pool spacing and bed slope (Table 2): large spacing ($L > 2.5B$) and high bed slope ($S_0 > 7\%$) did not produce hydraulic fields compatible with the fish swimming performance of cyprinids at higher flow rates ($Q > 1.28$ m^{3}s^{-1}, in series-B and C). Here, the series-A, D, E, F and G at a flow rate of 1.92 m^{3}s^{-1} or less (in prototype) achieve the requirements (Figure 8(b)). Similar to the findings for the first fatigue restriction, high pool spacing resulted in flow velocities that were too high to enable successful passage by salmonids for C5 ($L = 3B$) and cyprinids for C4–C5 ($L = 2.5$–$3B$) at all flow rates, whereas high bed slopes also resulted in failure for cyprinids in B4–B5 ($S_0 = 7\%$–10%) at all flow rates.

Table 2. Swimming performance of salmonid and cyprinid species for the second fatigue restriction.

Weir layouts	Series (simulation)	Flow rate[a] ($m^3 s^{-1}$)	Fish species (200-mm body length)	Second restriction* Successful	Second restriction* Unsuccessful
I	A	3.20	Salmonids	✓	
I	B1	2.88	Salmonids	✓	
I	B2–B4	1.92	Salmonids	✓	
I	B5	1.28	Salmonids	✓	
I	C1	2.88	Salmonids	✓	
I	C2–C3	1.92	Salmonids	✓	
I	C4	1.28	Salmonids	✓	
I	C5	1.28	Salmonids		✓
I	D1–D2	1.92	Salmonids	✓	
I	E1–E3	2.88	Salmonids	✓	
II	F	3.20	Salmonids	✓	
III	G	2.88	Salmonids	✓	
I	A	1.92	Cyprinids	✓	
I	B1–B2	1.92	Cyprinids	✓	
I	B3	1.28	Cyprinids	✓	
I	B4–B5	1.28	Cyprinids		✓
I	C1	1.92	Cyprinids	✓	
I	C2–C3	1.92	Cyprinids	✓	
I	C4–C5	1.28	Cyprinids		✓
I	D1–D2	1.28	Cyprinids	✓	
I	E1–E3	1.92	Cyprinids	✓	
II	F	1.92	Cyprinids	✓	
III	G	1.92	Cyprinids	✓	

[a]Maximum flow rate in prototype model (1:4 scale).
*$U_{eq} \leq 2.0$ ms^{-1} and $D_{max} \geq L$.

4. Design procedures

The design of a fishway consists of considering the most physical important factors, such as head-drop, slope, flow velocity and water depth (Baudoin et al. 2014), as well as the swimming performance and behaviour of the target fish species (Katopodis 1992). The hydraulic conditions in the fishway depend on channel geometry and flow through the fishway during migratory periods (Baudoin et al. 2014). The design performance of rock-weir fishways is discussed in the previous sections in the context of fish resting zones, volumetric dissipated power and fish swimming performance. These results suggest that the rock-weir fishways that are most hydraulically suitable to fish passage are oriented with "V" facing upstream (layout I), with bed slope $S_0 \leq 5.5\%$, pool spacing $0.5B < L \leq 2.5B$, weir height $d > 0.125$ m and arm angle $\theta \geq 60$ degrees. The other layouts (II: V-weir facing downstream III: crossbar block ramp) should only be considered for locations where fish prefer to swim along the channel banks (see Baki et al. 2017).

The following design steps for a rock-weir fishway are recommended for a definite channel assuming a design flow rate (Q):

1. Determine the channel bed slope (S_0) based on the elevation difference in the total project length, the number of rock-weir/pools and the pool spacing;
2. Estimate the preliminary rock-weir height (d, boulder height from the channel bed). Note that the pool spacing and rock-weir height in steps 1 and 2, respectively, are preliminary until depth and velocity criteria have been met, which will be verified by the recommended spacing and height for a specific weir layout by Baki et al. (2017);
3. Assume water depth above rock-weir crest (h) for specific pool spacing (L);
4. Approximate the pool average water depth (H) following the best fitted power relationship $H/d = 1.252(Q^*)^{0.552}$, developed based on simulated results for all flow regimes, where $Q^* = Q/\sqrt{gS_0 LB^2 \Delta h}$ is the dimensionless flow rate;
5. Estimate the values of $Q_t^* = Q/(\sqrt{(g)}S_0 BL^{3/2})$ and the ratios of L/d and H/d to identify the flow regime (weir, transitional or streaming) based on the quantitative thresholds recommended in Figure 6 by Baki et al. (2017);
6. Predict the flow rate through the fishway, $Q = C_d h^{1.15} B_t^{1.35} \sqrt{gS_0}$, where C_d is specific to the flow regime and acquired following Equation (7 or 8) from Baki et al. (2017);
7. Adjust h and repeat steps 3–6 until the design and computed discharges are equal, i.e. the target h is achieved;
8. Calculate maximum velocity U_{max} using Equations (9 and 10) from Baki et al. (2017) using the dimensionless $Q^* = Q/\sqrt{gS_0 LB^2 \Delta h}$ for the specific flow regime; and
9. Compare the estimated water depth and maximum flow velocity to the values appropriate to the target fish species; if these values are not suitable, then repeat steps 1–9 using a different pool spacing and rock-weir height.

The above design procedures are based on fishway hydraulics. In practise, design provisions and configuration requirements for a specific rock-weir fishway facility will depend on the site characteristics and should be monitored in the field to ensure fishway effectiveness.

5. Conclusions

This study numerically investigated the relationship between rock-weir hydraulics and fish passage for different channel and structure configurations. The generalized results through this modelling study can be extrapolated to prototype scale fishways using Froude number similarity analysis to better integrate requirements for fish migration in rock-weir NLFs design.

The rock-weir fishway simulations produced water depth and flow velocities suitable for fish passage under different channel characteristics and structure geometries. Sufficient slow velocity areas for fish resting in rock-weir fishways (i.e. zones where the velocity is less than $0.4U_{max}$ over 30% of the pool area) was created for bed slope $S_0 \leq 5.5\%$, pool spacing $L \leq 2.5B$ and weir height $d \geq 0.125$ m. The average volumetric energy dissipation rate is sensitive to both channel slopes and flow rates and is less influenced by the

boulder-weir geometry. For a full-scale prototype structure (1:4), the boulder-weir NLFs ensured flow fields low enough to be overcome by 200-mm long salmonids or cyprinids for bed slopes lower than 7% and specific pool spacing ($0.5B < L < 3B$ for salmonids and $0.5B < L < 2.5B$ for cyprinids).

The results of this study have advanced our knowledge of flow in a rock-weir fishway in the context of fish passage, and will be useful to engineers and fish biologists involved in the design of rock-weir fishways. Field testing of these design criteria should be conducted to validate model predictions and improve guidance on the criteria used to develop effective fishways.

Notation

The following symbols are used in this paper:

B	channel width
B_t	total wetted length of rock-weir crest
D_f	fish swimming distance
D_{max}	maximum fish swimming distance
d	rock-weir height above channel bed
E	average volumetric energy dissipation rate
g	gravitational acceleration
H	pool averaged water depth along the centre line of the channel
H_0	unregulated water depth referred to as normal depth
h	water depth above the rock-weir crest
Δh	difference in water level between two pools
k	turbulent kinetic energy
L	pool spacing
Q	flow rate, $m^3 s^{-1}$
Q^*	dimensionless discharge ($Q^* = Q/(\sqrt{gS_0 LB^2 \Delta h})$
Q_t^*	dimensionless discharge at transition($Q_t^* = Q/(\sqrt{(g)}S_0 B_t L^{3/2})$
S_0	channel slope
T	endurance time
U	magnitude of flow velocity considering three-directions ($U = \sqrt{u^2 + v^2 + w^2}$)
U_{max}	maximum value of U over weir
U_{eq}	equivalent constant water velocity along the fish path
U_{max}^*	dimensionless maximum velocity ($U_{max}^* = U_{max}/\sqrt{2gS_0 L}$)
V_0	pre-structure velocity referred to normal depth
V_p	volume of pool excluding the volume of rock-weir
z	vertical distance from the channel bed
θ	weir arm angle (plan view angle of departure from bankline)
ρ	the density of water
η	maximum velocity reduction factor in percent ($\eta = (V_0 - U_{max})/V_0 \times 100$)
ε	turbulent kinetic energy dissipation rate
a, b and c	coefficients

References

ANSYS CFX. 2015. Release 16.2. Canonsburg (PA): ANSYS Inc. p. 15317.

Baki ABM, Zhu DZ, Harwood A, Lewis A, Healey K. 2017. Rock-weir fishway. I: flow regimes and hydraulic. J Ecohydraul. doi.org/10.1080/24705357.2017.1369182.

Baki ABM, Zhu DZ, Rajaratnam N. 2014. Mean flow characteristics in a rock-ramp-type fish pass. J Hydraul Eng. 140(2):156–168.

Baki ABM, Zhu DZ, Rajaratnam N. 2016. Flow simulations in a rock-ramp-type fish pass. J Hydraul Eng. 142 (10):04016031.

Baudoin JM, Burgun V, Chanseau M, Larinier M, Ovidio M, Sremski W, Steinbach P, Voegtle B. 2014. Assessing the passage of obstacles by fish. Concepts, design and application. Vincennes (France): Onema.

Bell M. 1986. Fisheries handbook of engineering requirements and biological criteria. Fish passage development and evaluation program. Portland (OR): US Army Corps of Engineers, North Pacific Division Portland.

Castro-Santos T. 2005. Optimal swim speeds for traversing velocity barriers: an analysis of volitional high-speed swimming behavior of migratory fishes. J Exp Biol. 208:421–432.

Comiti F, Cadol D, Wohl E. 2009. Flow regimes, bed morphology, and flow resistance in self-formed step-pool channels. Water Resour Res. 45:Wo4424.

Cox A. 2005. A study of in-stream rehabilitation structures in sand-bed channels [M.S. dissertation]. [Fort Collins (CO)]: Colorado State University.

Deutscher Verband für Wasserwirtschaft und Kulturbau e.V. [DVWK]. 2002. Fish passes – design, dimensions and monitoring. Rome: Food and Agriculture Organization of the United Nations in arrangement with German Association for Water Resources and Land Improvement as DVWK-Merkblatt.

Franklin AE, Haro A, Castro-Santos T, Noreika J. 2012. Evaluation of nature-like and technical fishways for the passage of Alewives at two coastal streams in New England. Trans Am Fish Soc. 141:624–637.

Hammer C. 1995. Fatigue and exercise tests with fish. Comp Biochem Physiol: Physiol. 112(1):1–20.

Katopodis C. 1992. Introduction to fishway design. Winnipeg (MB): Working Document, Fisheries and Oceans Canada, Freshwater Institute.

Katopodis C, Gervais R. 2012. Ecohydraulic analysis of fish fatigue data. River Res Appl. 28(4):444–456.

Katopodis C, Williams JG. 2011. The development of fish passage research in a historical context. Ecol Eng. 48:8–18.

Larinier M. 2008. Fish passage experience at small-scale hydro-electric power plants in France. Hydrobiologia. 609:97–108.

Puertas J, Cea L, Bermudez M, Pena L, Rodriguez A, Rabunal JR, Balairon L, Lara A, Aramburu E. 2012. Computer application for the analysis and design of vertical slot fishways in accordance with the requirements of the target species. Ecol Eng. 48:51–60.

Rosgen DL. 2001. The cross vane, W-weir and J-hook structures: their description, design and application for stream stabilization and river restoration. Proceedings of the Wetland Engineering and River Restoration Conference; 2001 Aug 27–31; Reno (NV). Reston (VA): ASCE.

Thomas D, Abt S, Mussetter R, Harvey M. 2000. A design procedure for sizing step-pool structures. Proceedings of the Joint Conference on Water Resource Engineering and Water Resources Planning and Management; 2000 Jul 30–Aug 2; Minnesota, USA. Reston (VA): ASCE.

Toombes L. 2002. Experimental study of air-water flow properties on low-gradient stepped cascades [PhD dissertation]. [Brisbane (Australia)]: University of Queensland.

Towler B, Mulligan K, Haro A. 2015. Derivation and application of the energy dissipation factor in the design of fishways. Ecol Eng. 83(10):208–217.

Wang RW, David L, Larinier M. 2010. Contribution of experimental fluid mechanics to the design of vertical slot fish passes. Kwol Manag Aquat Ecosyst. 396(02):1–21.

Wu S, Rajaratnam N, Katopodis C. 1999. Structure of flow in vertical slot fishway. J Hydraul Eng. 125(4):351–360.

Yagci O. 2010. Hydraulic aspects of pool-weir fishways as ecologically friendly water structure. Ecol Eng. 36:36–46.